

**CLINICAL ASSESSMENT OF LEFT  
VENTRICULAR REGIONAL CONTRACTION  
PATTERNS AND EJECTION FRACTION BY  
HIGH-RESOLUTION GATED SCINTIGRAPHY**

Daniel S. Berman, Antone F. Salel, Gerald L. DeNardo, Hugo G. Bogren, and Dean T. Mason

*University of California School of Medicine at Davis, Davis,  
and Sacramento Medical Center, Sacramento, California*

*An improved, noninvasive, radionuclidic, gated blood-pool imaging technique has been developed for clinical analysis of regional contraction abnormalities of the left ventricle and determination of ejection fraction. The principal innovations include high-resolution collimation, higher information density, improved method for dynamic aortic-mitral-diaphragmatic border delineation, accurate selection of the end-systolic gating interval through the use of the phonocardiogram, and accurate end-diastole by on-line gating immediately following the electrocardiographic QRS. The results of scintigraphic studies were compared with selective radiopaque cineangiographic findings in 27 patients with cardiac disease; excellent correlations of ejection fractions ( $r = 0.93$ ) and abnormal contraction patterns (17/17 patients) were demonstrated. In addition, the clinical usefulness in evaluating ventricular performance was demonstrated in 79 patients with acute and chronic coronary artery disease. This radionuclidic technique allowed assessment of reversibility of segmental dyssynergy by the response to nitroglycerin in 20 patients. These findings demonstrate the validity of this improved radionuclidic technique in the atraumatic quantification of ventricular function and suggest its usefulness in a variety of clinical conditions.*

Left ventricular ejection fraction and regional myocardial contraction patterns are important parameters of cardiac pump performance which, until recently, have required invasive procedures for measurement. The Anger scintillation camera has been used in the development of the atraumatic technique of radioisotopic angiography (1,2). In

1971, Strauss, et al (3,4) used gated cardiac blood-pool imaging to assess ejection fraction and segmental contraction. Despite the value of their technique, difficulties with precise delineation of the left ventricular silhouette were evident. Ejection fraction can also be measured by employing scintillations obtained from an area of interest encompassing the left ventricular chamber (5-9) but this area-counts method fails to provide information regarding patterns of regional contraction. Since the earliest abnormality of cardiac pump function in coronary atherosclerosis is disturbance of the orderly sequence of systolic motion (ventricular dyssynergy) (10,11), the gated blood-pool technique offers greater sensitivity than the area-counts method in the identification of ischemic heart disease.

The present study describes improvements in the radionuclidic gated blood-pool imaging technique that enhance delineation of cardiac margins by using a high-resolution collimator, greater information density, and phonocardiographic definition of gated intervals of the cardiac cycle. The validity of this improved imaging technique is established by correlation with selective left ventricular cineangiography performed on 27 patients with a variety of cardiac disorders. Further, the practicality and usefulness of this noninvasive scintigraphic method in directing clinical decisions is illustrated by selected examples from our experience with 79 patients.

**MATERIALS AND METHODS**

**Patients.** Correlative scintigraphic and cineangiographic studies were performed on 27 adults: 22 with

Received Dec. 12, 1974; revision accepted April 22, 1975.

For reprints contact: Daniel S. Berman, Section of Nuclear Medicine, University of California School of Medicine, Davis, Calif. 95616.

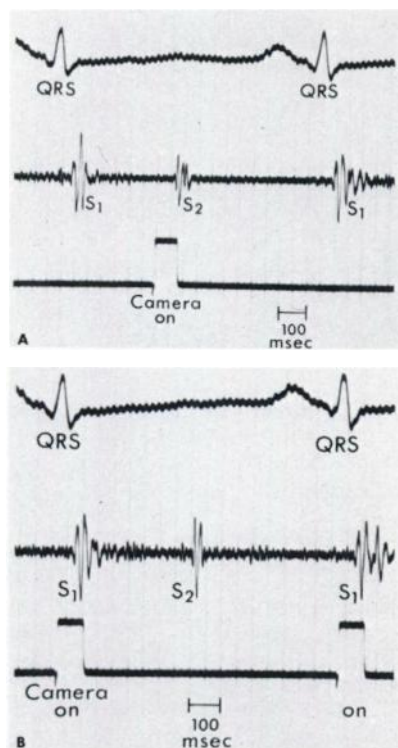


**FIG. 1.** Recording in patient with coronary disease showing simultaneous phonocardiographic (middle) and electrocardiographic (top) tracings utilized to determine end-systolic gating interval (camera on) (A) and end-diastolic gating interval (camera on) (B). S<sub>1</sub> is first heart sound; S<sub>2</sub> is second heart sound.

coronary heart disease, 4 with rheumatic mitral regurgitation, and 1 with idiopathic hypertrophic sub-aortic stenosis. The radionuclidic and radiopaque studies were randomly sequenced and performed within 18–24 hr of each other.

In addition, cardiac scintigraphy was utilized to evaluate ventricular performance in an additional 40 patients with acute and chronic coronary artery disease as part of their clinical management.

**Radionuclidic methods.** The radionuclidic imaging technique formulated in this investigation comprised several modifications of the gated blood-pool method initially described by Strauss, et al (3,4). The principal innovations characterizing our new method consisted of: (A) use of a 16,000-hole high-resolution low-energy collimator; (B) higher information density; (C) improved delineation of the diaphragmatic border of the left ventricle by discrimination of this chamber from the right ventricle; (D) determination of mitral and aortic valve annular motion; (E) accurate selection of the end-systolic gating interval through the use of the phonocardiogram; (F) accurate end-diastolic gating governed on-line by the ventricular depolarization activating the subsequent contraction; and (G) employment of a videotape data store playback system for development of selected temporal

segments of the first pass of the radioactive bolus through the right and left heart chambers.

**Preparation.** The patient was placed supine in the 30-deg right anterior oblique (RAO) position beneath the scintillation camera detector (Searle Radio-graphics Pho/Gamma HP) equipped with a 16,000-hole high-resolution low-energy collimator. The heart was positioned in the detector's field of view by transmission scanning while the location of the cardiac image was observed on the persistence oscilloscope. The phonocardiogram was obtained at the second left parasternal intercostal space. The end-systolic gating interval was determined before scintillation imaging and consisted of the 60-msec interval immediately preceding the first high-frequency component of the second heart sound signifying aortic valve closure and termination of left ventricular ejection. The gate control of the gating device was programmed to unblank the oscilloscope for a 60-msec interval. The delay control of the R wave-triggered gating apparatus was advanced until the 60-msec gated interval occurred immediately before the subsequent aortic closure sound (Fig. 1A). End-diastole was chosen as the 60-msec interval immediately after the electrocardiographic R wave and was obtained by setting the delay control at zero. Thus, the 60-msec end-diastolic interval always occurred immediately after the QRS and was independent of the R-R interval (Fig. 1B).

**Procedure.** Fifteen to twenty millicuries of <sup>99m</sup>Tc-human serum albumin (12) or <sup>99m</sup>Tc-autologous red blood cells (13) contained in a volume of less than 1.5 cc was injected as a bolus through a short plastic catheter previously placed in an antecubital vein. The scintigraphic data occurring during the initial 1 min after injection were collected ungated on videotape for subsequent validation of the location of the aortic and mitral annuli. After the first minute, the gating device with the preset delay for end-systole was activated. A 500,000-count image of end-systole was obtained on Polaroid film from the summation of counts during 500–1,000 systoles that usually required 10 min (Fig. 1A). The delay control of the gating apparatus was then switched to zero and a 500,000-count image of end-diastole was obtained (Fig. 1B) in an additional 10 min. Linear calibration was accomplished by placing a ruler with parallel strips of lead 1-cm wide and spaced 1-cm apart on the collimator face and obtaining a 500,000-count image by placing a sheet source containing <sup>99m</sup>TcO<sub>4</sub> behind the lead grid.

The scintigraphic data obtained in the first minute were utilized to expose serial 1-sec Polaroid images of the movement of the radioactive bolus through the heart during the initial circulation. These 1-sec

images were obtained for the precise timing of the right and left heart phases. Images of these phases of the initial transit of the radioactive bolus were obtained by single replay of the videotape for the selected time intervals. Each of the right and left heart images contained about 100,000 counts.

**Interpretation.** The borders of the left ventricle were outlined on the end-systolic and end-diastolic films with a paraffin pencil. In 18 of the 27 patients all margins of the left ventricle, including the aortic and mitral valve planes, were determined by inspection of the end-systolic and end-diastolic gated images. In these 18 patients the information from the images obtained from the initial passage of the bolus through the heart was used to verify further the accuracy of placement of the mitral and aortic borders. In the other nine patients it was necessary to use the initial transit image of the left ventricle to determine the aortic and mitral valve planes.

Transparent photographs (35 mm) of the outlined end-systolic and end-diastolic images and of the lead ruler image were made. The images of the cardiac chambers were projected to life size by using the lead ruler for calibration. Through the use of a central artifact produced by the gating device, the images of systole and diastole could be superimposed accurately. The outlines of the left ventricle in systole and diastole were traced onto paper placed over the projection screen. The superimposed images of systole and diastole were inspected for evidence of regional abnormalities of the contraction pattern (14). The areas (A) of the traced chamber images were measured by planimetry. The long axis (L) of the inner surface of the left ventricle was measured from the mid-aortic valve plane to the apex. End-systolic and end-diastolic left ventricular volumes were calculated utilizing the area-length formula  $V = 0.849A^2/L$  based on the standard equation of Sandler, et al (15) which assumes that the left ventricle is a prolate spheroid. The scintigraphic ejection fraction was then calculated by dividing the stroke volume (end-diastolic volume less end-systolic volume) by the end-diastolic volume.

**Reproducibility.** The reproducibility of the improved scintigraphic method was assessed by studying two patients with chronic ischemic heart disease on two occasions separated by a 48-hr interval to allow for radionuclidic decay. One patient had normal sinus rhythm, and the other was purposely selected as a severe test of the method because of the presence of marked congestive heart failure and atrial fibrillation. Since the systolic time interval varies from beat to beat in atrial fibrillation, accurate end-systolic timing is difficult.

**Left anterior oblique view.** In selected patients,

gated left ventricular imaging was performed in the modified left anterior oblique (MLAO) position (16). The MLAO images in end-systole and end-diastole were obtained immediately after the RAO gated images were recorded. The MLAO images were used particularly to evaluate interventricular septal and posterior wall motion.

**Pharmacologic intervention.** In 20 patients with coronary artery disease the reversibility of segmental dyssynergy was determined from RAO end-systolic and end-diastolic gated images obtained immediately preceding and following the administration of nitroglycerin, 0.4–0.6 mg sublingually. The phonocardiographically determined end-systolic gating interval was adjusted for the drug-induced increase in heart rate.

**Radiopaque methods.** Selective left ventricular cineangiography was performed in the 30-deg right and 60-deg left anterior oblique projections on 35-mm film taken at 64 frames/sec using a Philips 9-in. image amplifier system. The ventricle was opacified with 50–75 cc of Hypaque-M®, 75% containing sodium and meglumine diatrizoates injected at 300–400 lb/in.<sup>2</sup> through a catheter. Tracings of the left ventricular end-diastolic and end-systolic endocardial silhouettes were obtained in the RAO position from which determinations of ventricular volumes and segmental contraction were performed (14). The first complete cardiac cycle in which the left ventricular cavity was completely opacified by contrast material, and which was at least two beats following any premature ventricular contractions, was utilized for the end-systolic and end-diastolic images. End-systolic volume, end-diastolic volume, and ejection fraction were determined with the same formulas used in the radionuclidic method (15).

## RESULTS

**Ejection fraction and regional contraction patterns; comparison of high-resolution scintigraphy with contrast cineangiography.** In the 27 patients constituting the principal comparative group (Table 1) the mean absolute difference was 8%. The mean ratio of the radioisotopic and radiopaque determinations was 0.98 indicating lack of bias. The results are displayed graphically in Fig. 2. The correlation coefficient was 0.93 ( $p < 0.001$ ). In 14 of the 22 patients with coronary heart disease, left ventricular gated scintigraphy and cineangiography demonstrated regional abnormalities of wall motion in individual patients that were similar in location, nature, and extent by both techniques. These 14 patients included 1 with diaphragmatic hypokinesis; 8 with predominant apical hypokinesis, akinesis, or dyskinesis; 3 with predominant anterior free wall hypo-

**TABLE 1. COMPARISON OF RADIOISOTOPIC AND RADIOPAQUE LEFT VENTRICULAR EJECTION FRACTIONS**

Patient	Diagnosis	Ejection fraction		Difference (%)
		Radio-isotopic	Radiopaque	
WL	CAD	0.84	0.80	+5
VN	MR	0.83	0.90	-8
DB	CAD	0.71	0.68	+4
EQ	CAD	0.74	0.71	+4
SL	CAD	0.56	0.76	-26
WH	CAD	0.61	0.55	+11
HK	CAD	0.57	0.57	0
GD	CAD	0.65	0.68	-4
LA	CAD	0.74	0.79	0
JA	CAD	0.79	0.77	+3
EK	CAD	0.55	0.52	+6
RP	CAD	0.67	0.66	+2
PD	MR	0.57	0.56	+2
PL	CAD	0.82	0.80	+3
EH	CAD	0.85	0.73	+16
JR	CAD	0.71	0.65	+9
TH	CAD	0.60	0.60	0
WC	MR	0.39	0.41	-5
CG	CAD	0.71	0.74	-4
RD	IHSS	0.85	0.84	+1
WF	CAD	0.21	0.36	-42
RP	CAD	0.37	0.50	-26
JV	CAD	0.76	0.85	-11
EP	CAD	0.47	0.49	-4
RD	CAD	0.56	0.58	-3
LV	CAD	0.17	0.16	+6
VB	MR	0.42	0.41	+2

Abbreviations: CAD is coronary artery disease, MR is mitral regurgitation, and IHSS is idiopathic hypertrophic subaortic stenosis.

kinesis or akinesis; and 2 with combinations of these abnormalities. The remaining eight patients with coronary disease exhibited normal contraction patterns by both scintigraphy and cineangiography; none of these patients had electrocardiographic evidence of previous myocardial infarction. Of the other five patients with cardiac disorders, three with rheumatic disease demonstrated generalized hypokinesis by both studies. One additional patient with rheumatic disease and the one patient with idiopathic hypertrophic subaortic stenosis had normal contraction patterns on the radionuclidic and radiopaque examinations. Seven of the 14 patients with coronary artery disease and regional dyssynergy had normal ejection fractions ( $>0.60$ ).

**Reproducibility of high-resolution scintigraphy.** In the patient with normal sinus rhythm who underwent repeat radionuclidic gated imaging, the ejection fractions were 0.55 and 0.52, and anterior apical hypokinesis was detected on the two examinations. In the patient with atrial fibrillation, the sequential ejection fractions were 0.39 and 0.42 and apical akinesis was demonstrated on both occasions. In

this patient who also underwent cineangiography, the ejection fraction was 0.42 by contrast dye analysis.

**Timing of end-systole and end-diastole.** Accurate delineation of end-systole and end-diastole during scintigraphy was achieved in all 27 patients. Phonocardiography enabled precise end-systolic gating in each individual despite the presence in five patients of flat T waves in all of the 12 standard electrocardiographic leads (Fig. 1A). Concerning end-diastole, accurate gating was achieved in all patients, irrespective of cardiac rhythm, by triggering the gating device with the R wave and imaging immediately (zero delay) (Fig. 1B).

**Delineation of left ventricular borders.** Use of the high-resolution collimator and exposures consisting of 500,000 recorded events improved image resolution and thereby enhanced certainty of the location of the borders of the left ventricle. The improved border definition was particularly helpful in defining the aortic, mitral, and diaphragmatic margins of the left ventricle that have been difficult to discern with previous radioisotopic techniques. In 18 of the 27 patients, therefore, the medial left ventricular margin was defined by inspection of the gated images that revealed a line of decreased activity representing the atrioventricular groove, and the region of the aortic annulus (Fig. 3). Using the atrioventricular groove to draw the medial left ventricular margin in systole and diastole, it was possible to include movement of this portion of the left ventricle in the end-systolic and end-diastolic images in the calculation of ejection fraction. Movement of this margin noted in the radionuclidic study was confirmed by similar motion of these structures on the radiopaque angiogram (Fig. 3). In the 18 patients in whom the atrioventricular groove was visualized, the summation images of the

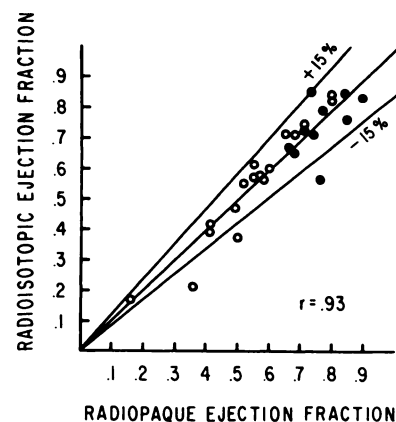


**FIG. 2.** Comparison of left ventricular ejection fraction measurements obtained by radioisotopic and radiopaque methods in 27 patients. Closed circles are normal contraction pattern; open circles are abnormal contraction pattern. Center line is line of identity and outer lines represent 15% distribution limits.

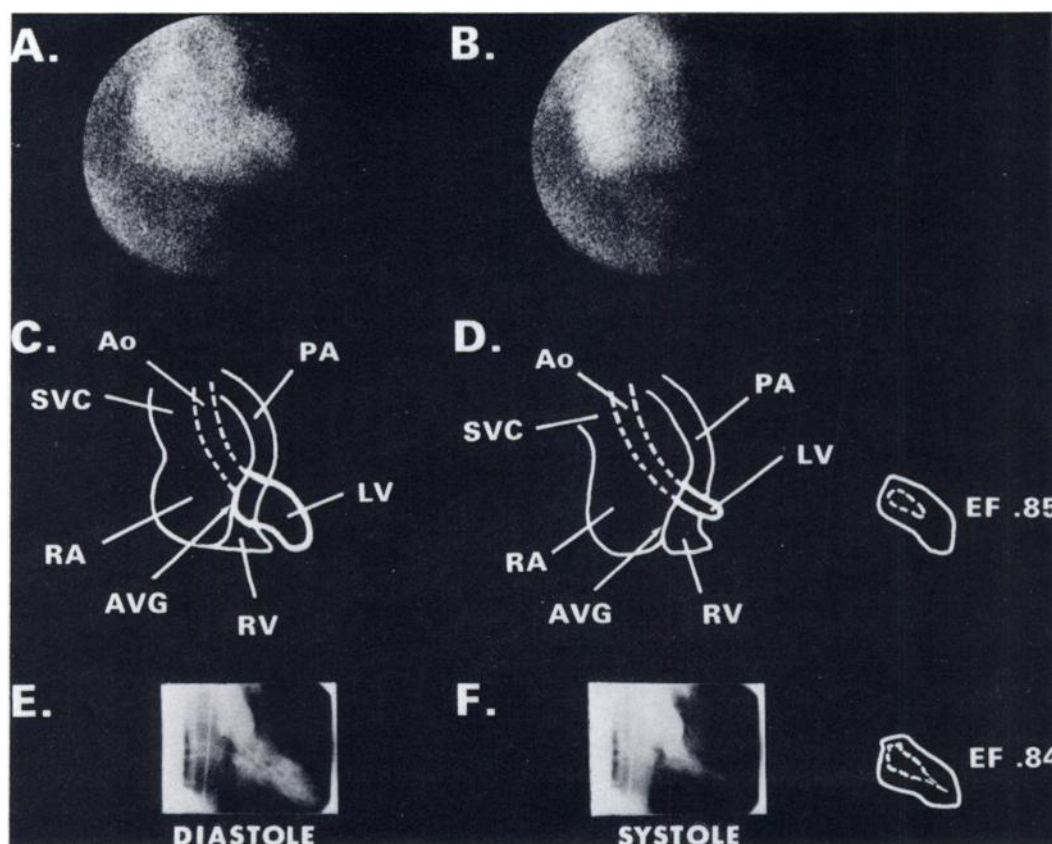


**FIG. 3.** Scintigraphic images (A and B) in right anterior oblique view (RAO) in Patient RD with idiopathic hypertrophic subaortic stenosis demonstrating improved method for delineating left ventricular margins (thick lines of diagrams C and D) afforded by high-resolution technique. Comparative left ventricular cineangiograms in same patient are shown (E and F). Left column (A, C, and E) is at end-diastole and middle column (B, D, and F) is at end-systole. Diagrams in right column display superimposed end-

diastolic (solid lines) and end-systolic (broken lines) outlines of left ventricle obtained from radioisotopic (top) and radiopaque (bottom) images. EF is ejection fraction, SVC is superior vena cava, RA is right atrium, RV is right ventricle, PA is pulmonary artery, LV is left ventricle, Ao is ascending aorta, and AVG is atrioventricular groove. Systolic obliteration of apical portion of left ventricular cavity is evident.

left ventricular phase from the initial ungated portion of the scintigraphic study served as an internal check on placement of this margin. In the other 9 of the 27 patients this region could not be precisely identified by inspection of the gated images alone. In these patients the summation images of the left and right heart phases derived from the initial transit of the radioactive bolus through the heart were used to outline the mitral and aortic planes which were then considered stationary during the cardiac cycle.

The diaphragmatic border of the left ventricle was also more clearly defined in our technique. In most patients, the right ventricle extended beneath the left ventricle in the RAO position. Because of the high-resolution collimator and high information density, it was usually possible to observe a line of decreased activity separating the diaphragmatic border of the left ventricle from the right ventricle. This line was used for drawing the left ventricular outline in systole and diastole (Fig. 3).

**Clinical illustrations.** Since the establishment of the validity of this radionuclidic method, the procedure has been applied in a variety of clinical settings

for the noninvasive assessment of ventricular pump function. The following examples illustrate the clinical usefulness of this technique.

The value of the method in evaluating the viability of abnormally contracting ventricular segments in ischemic heart disease is shown by the scintigraphic images obtained before and after the sublingual administration of nitroglycerin in Patient TH who had preinfarction angina pectoris (Fig. 4). On the radionuclidic (Fig. 4C and D) and contrast (Fig. 4A and B) images obtained before the administration of nitroglycerin, hypokinesis of the left ventricular apex was evident; coronary angiography demonstrated 90% stenosis of the left anterior descending coronary artery. Following nitroglycerin administration, the extent of apical inward motion during ejection became normal, and the ejection fraction increased (Fig. 4E and F), thereby indicating the area of dyssynergy was ischemic rather than infarcted. Based on this information, aorto-coronary saphenous vein bypass rather than segmental resection was performed.

The radionuclidic procedure has also been used



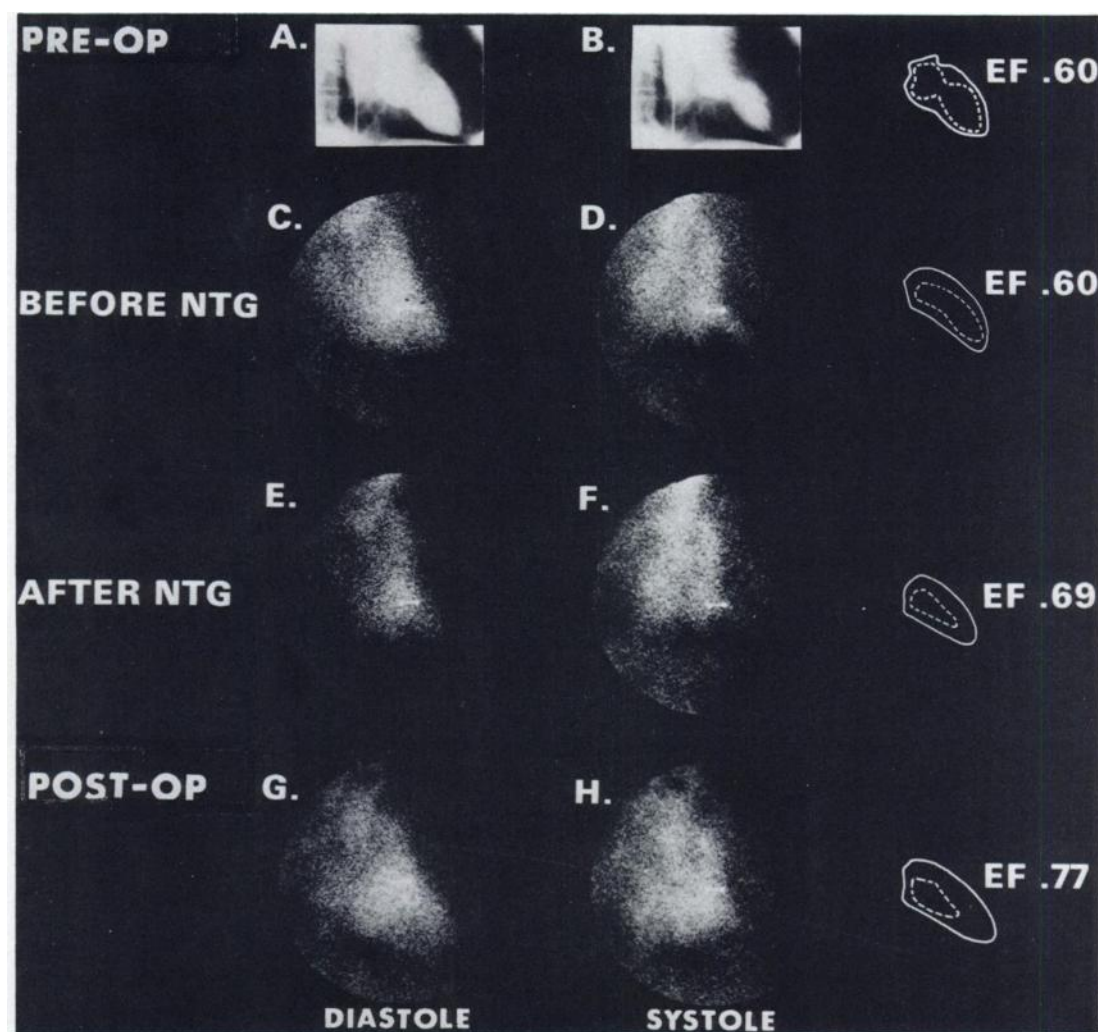


**FIG. 4.** Scintigraphic images obtained before (C, D) and after (G, H) coronary artery bypass surgery in Patient TH with preinfarction angina pectoris. Also shown are preoperative scintigraphic images obtained after sublingual nitroglycerin (NTG) (E and F). Preoperative left ventricular cineangiograms before NTG are shown in A and B. Superimposed end-diastolic and end-systolic outlines

and ejection fractions are given in right column. Before operation, hypokinesis of left ventricular apex is evident on radiopaque (A and B) and radionuclidic (C and D) images. Systolic movement of hypokinetic left ventricular apex (D) was improved after NTG (F), thereby indicating ischemia rather than infarction. After operation marked improvement in systolic apical motion is demonstrated (H).

to assess pump function following surgical coronary revascularization. In Patient TH described in the previous paragraph, gated scintigraphy performed 2 weeks postoperatively revealed normal apical wall motion during systole and improved ejection fraction (Fig. 4G and H). By using the radionuclidic technique, the efficacy of the revascularization operation was objectively documented without cardiac catheterization.

In addition, the radionuclidic technique may be applied in patients with chronic coronary disease and refractory heart failure in evaluating the feasibility of segmental myocardial resection. This application is illustrated by Patient LV who had diffuse hypokinesis of the entire left ventricle and a severely depressed ejection fraction (Fig. 5). It was determined that this patient was unsuitable for cardiac operation.

The scintigraphic method has been useful in evaluating abnormalities of the septal and posterior areas of the left ventricle by performing gated imaging in the MLAO position after completion of the RAO images. A striking example of the diagnostic capabilities of this procedure is shown by the RAO and MLAO images obtained in Patient RD who had idiopathic hypertrophic subaortic stenosis (IHSS) (Figs. 3 and 6). Obliteration of the left ventricular cavity characteristic of this entity is shown in the RAO image (Fig. 3B) and the asymmetrically thickened superior septal mass typifying IHSS (17,18) is clearly documented in the MLAO picture (Fig. 6B).

#### DISCUSSION

The radionuclidic, gated, cardiac blood-pool imaging technique was found to be an accurate, non-invasive method for the measurement of ejection

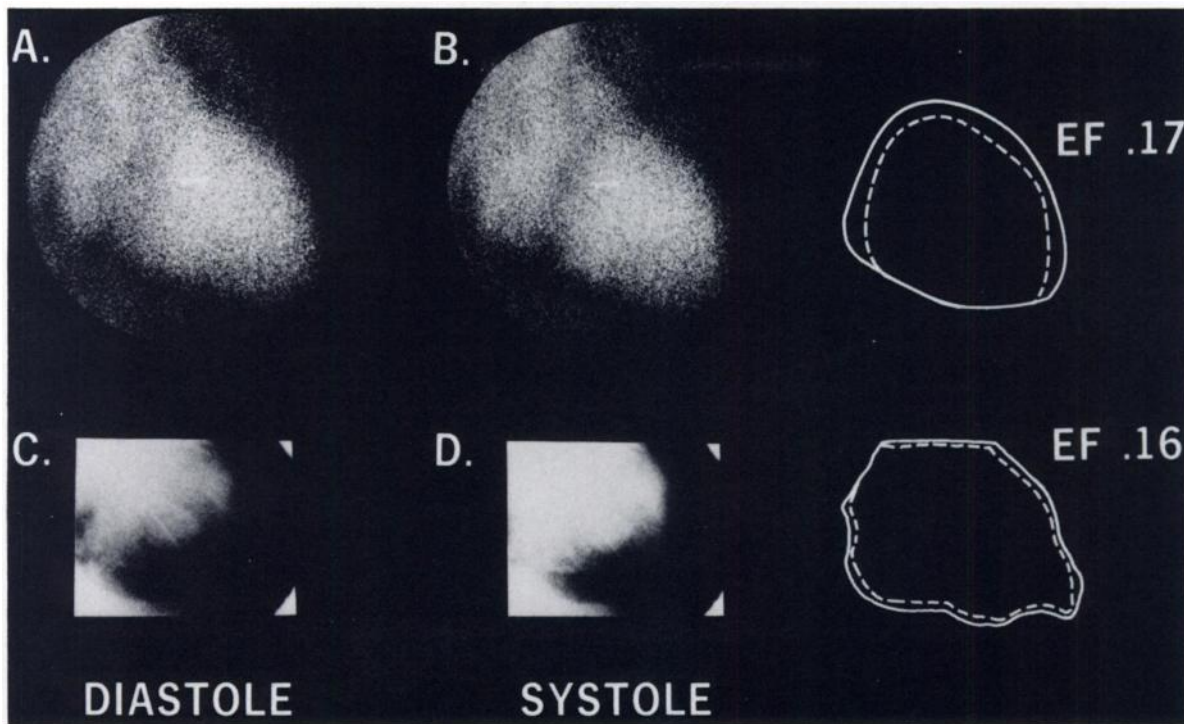


**FIG. 5.** Scintigraphic images obtained at end-diastole (A) and at end-systole (B) in Patient LV with chronic coronary heart disease; left ventricular angiograms are shown (C) and (D). Generalized

hypokinesis and akinesis of the entire left ventricular chamber is evident.

fraction and the evaluation of regional ventricular contraction patterns, thereby extending previous observations (3,4). Furthermore, the precision of this gated blood-pool approach was enhanced by several modifications of the earlier techniques. Image clarity was augmented by high-resolution collimation with greater information density, and end-diastole and end-systole were more accurately timed by using the phonocardiogram and related gating innovations.

Compared with earlier studies performed in this laboratory with the high-sensitivity collimator, marked improvement in image definition was achieved with the high-resolution collimator (Fig. 7). This improvement in image resolution is due to the greater depth of this collimator as compared with the high-sensitivity collimator; the greater depth minimizes degradation of resolution with increasing source-to-detector distances. This collimator characteristic is of special importance in RAO cardiac imaging in which the heart lies several inches from the detector.

The enhanced image resolution afforded by our technique provided clearer demarcation of the left ventricular outline, particularly in the regions of the mitral and aortic annuli and the diaphragmatic border. Moreover, our technique allowed detection of systolic movement of the aortic and mitral valve planes which has not been possible by previous RAO

gated blood-pool methods (3,4). Appreciation of valve plane motion at the base of the left ventricle is of special significance in ischemic heart disease, since excursion of this region may constitute the principal segmental inward motion of the chamber in patients with anterior and apical wall disease (10,11,14).

The improved delineation of the diaphragmatic border of the left ventricle in the present method made it possible to distinguish the diaphragmatic border of the left ventricle from the right ventricle. Using high-resolution collimation, we observed that the inferior margin of the right ventricle was located beneath the diaphragmatic border of the left ventricle in the majority of patients whereas, with methods providing lesser resolution, the apparent inferior left ventricular outline often represented the lower border of the right ventricle (3,4). Since the right ventricle moves inward with contraction and the inferior margin of this chamber does not greatly enlarge the combined ventricular silhouette in the RAO position, inability to differentiate the two chambers in this view does not markedly disturb estimation of ejection fraction; however, dyssynergy of the medial-inferior segment of the left ventricle may not be identified. Detection of abnormal motion in this region is identified by the high-resolution technique.

Concerning delineation of gating intervals, phono-

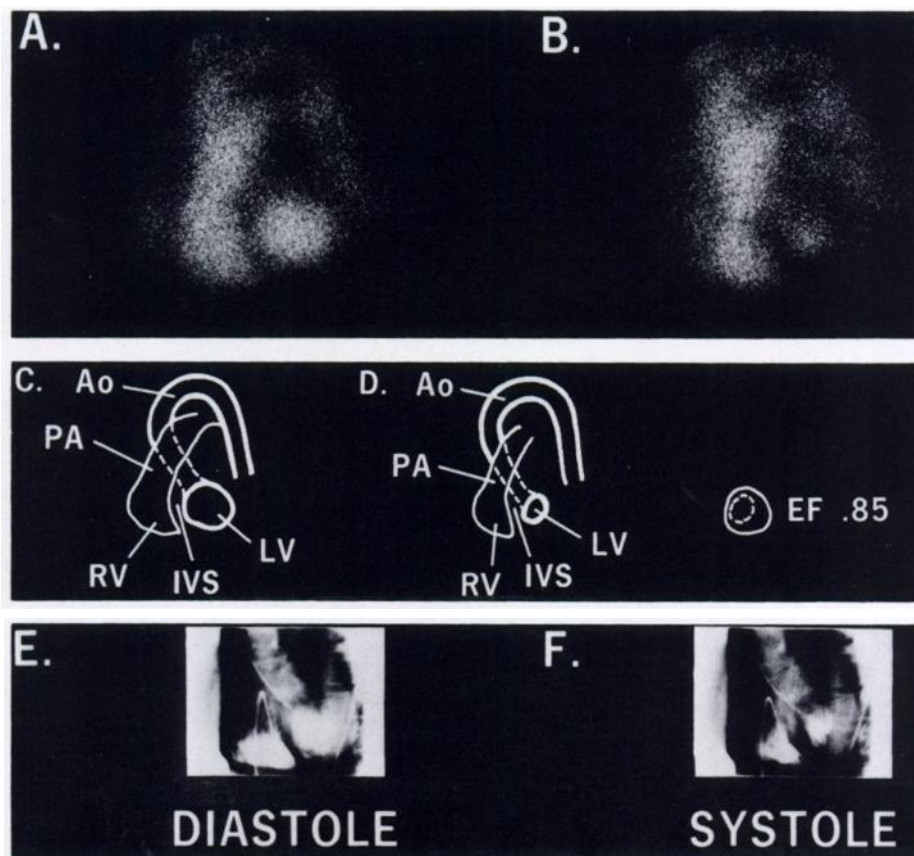


**FIG. 6.** Scintigraphic images in modified left anterior oblique view (LAO) obtained at end-diastole (A) and at end-systole (B) in Patient RD with idiopathic hypertrophic subaortic stenosis shown in Fig. 4. Diagrams drawn from the radionuclidic images are given

(C and D) and biventricular cineangiograms are illustrated (E and F). Asymmetrical thickening of interventricular septum (IVS) is clearly documented.

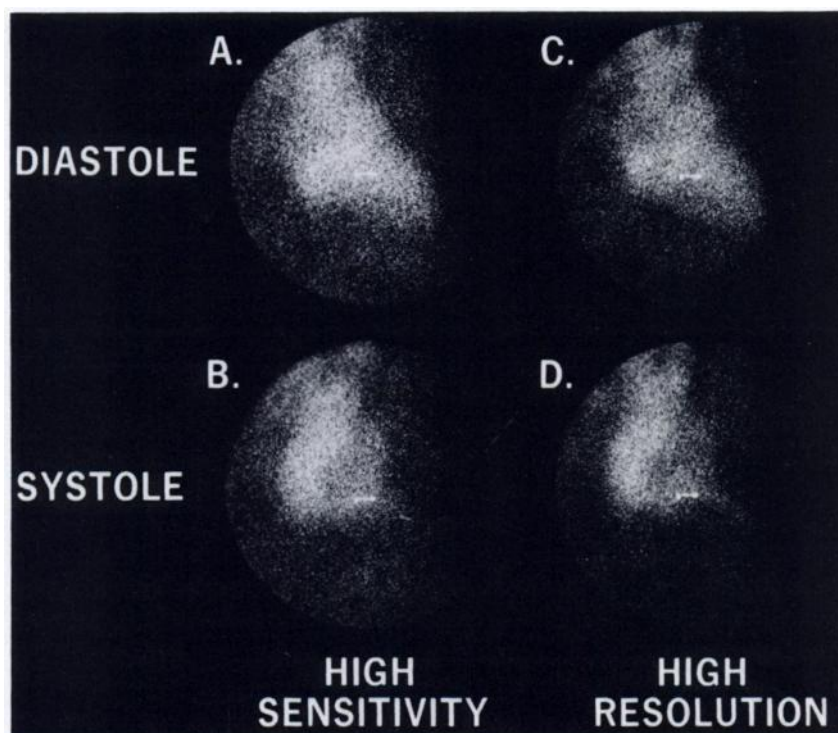


**FIG. 7.** Comparison of radionuclidic gated images obtained with high-sensitivity (A and B) and high-resolution (C and D) collimators in patient with coronary disease.



cardiography provided a means of improving the accuracy of end-systolic timing (Fig. 1A). This innovation is an advance over methods which utilize the terminal portion of the electrocardiographic T wave for estimating end-systole, since the T wave is often isoelectric in patients with heart disease (Fig. 1) (14). Furthermore, the electrical T wave may not precisely correspond to end-systole which is a mechanical event (19). This problem of non-coordination between electrical and mechanical events is particularly pronounced in patients with intraventricular conduction defects.

With regard to end-diastolic gating, some of the previous methods that employ gated imaging during the electrocardiographic PR interval triggered by a predetermined interval of delay from the preceding R wave are inaccurate (3,4), since imaging occurs during rather than at the end of atrial contraction (19). Furthermore, the timing becomes imprecise with small changes in heart rate and is invalid in atrial fibrillation. The method of end-diastole timing using triggering by the R wave with zero delay (Fig. 1B) obviates all of the above disadvantages of the PR interval gating method. Other methods of employing the R wave for end-diastolic timing have been described previously (7,20).

Thirty minutes were required for the method described here, but the procedure was well tolerated even by ill patients. The derived gated scintigrams represent average images of end-systole and end-diastole which could become distorted by patient movement during the time needed to obtain 500,000-count pictures with the higher resolution collimator. However, the time required for the study has recently been reduced by one-half by using a gating device (Riverside Bio-Engineering Model 901) that allows simultaneous imaging of end-systole and end-diastole on a single oscilloscope. Alternatively, the time of study can be shortened by recording the scintigraphic data ungated on videotape for subsequent retrieval of gated images (1,2,20).

In the past few years, a number of approaches have been developed for the radioisotopic determination of ejection fraction (2,3,5-9,20). Conceptually, these methods can be categorized as imaging (2,3,20) or area-counts (5-9) techniques; each can be performed utilizing initial transit (2,5,6,8,9,20) or static blood-pool (3,7) scintigraphic data. While correlation of each of these four methods with radiopaque cineangiography has been relatively good (3,5-9,20), there are certain advantages and limitations for each technique. The principal advantage of the imaging techniques is that the regional contraction pattern of the left ventricle can be observed in addition to ejection fraction. The ability to assess

segmental contraction as well as ejection fraction provides considerably greater sensitivity in detecting ischemic heart disease at an early stage (10,11,14). The importance of the ability of scintigraphic imaging to identify regional ventricular dyssynergy was clearly demonstrated in the present study in which 7 of 17 patients with normal ejection fractions manifested regional contraction abnormalities (Fig. 2).

One of the unique features of the gated blood-pool imaging technique is that the effects of pharmacologic and other interventions on ejection fraction and segmental motion can be determined by repeated imaging without additional injection of radiopharmaceutical or time elapse for radionuclidic decay. Clinical application of this feature was illustrated in the present investigation by evaluating the reversibility of abnormally contracting segments of the left ventricle in ischemic heart disease through scintigraphic observation of the response of these areas to nitroglycerin (Fig. 4). In addition, the usefulness of serial scintigraphy in the evaluation of the feasibility and efficacy of coronary bypass surgery was shown by preoperative assessment of segmental response to nitroglycerin and postoperative radionuclidic imaging (Fig. 4). It must be noted that although repeated imaging is easily performed after the intervention, providing immediate qualitative information about segmental wall motion changes, the interpreter must then spend time in determining the quantitative ejection fractions by the method described.

Finally, certain advantages would result from the combination of the initial transit area-counts method with the gated blood-pool imaging technique. The initial transit area-counts method would provide determination of ejection fraction; subsequently, the gated end-systolic and end-diastolic images can be obtained without additional radiopharmaceutical for evaluation of regional wall motion. In this manner, the major advantages of the initial transit area counts and imaging approaches can be combined in a single study of ejection fraction and regional myocardial contraction patterns.

#### ACKNOWLEDGMENT

The authors gratefully acknowledge the assistance of Anne-Line Jansholt, MS-Radiopharmacy, who developed the  $^{99m}\text{Tc}$ -albumin and  $^{99m}\text{Tc}$ -red blood cell radiopharmaceuticals. The technical assistance of Robert Kleckner is also gratefully acknowledged.

This work was supported in part by Research Program Project Grant HL-14780 from the National Heart and Lung Institute, National Institutes of Health, Bethesda, Md.

This work was presented in part at the Twenty-first Annual Meeting of The Society of Nuclear Medicine, San Diego, California, June 1974.

## REFERENCES

1. MASON DT, ASHBURN WL, HARBERT JC, et al: Rapid sequential visualization of the heart and great vessels in man using the wide field Anger scintillation camera. Radioisotope-angiography following the intravenous injection of technetium-99m. *Circulation* 39: 19-28, 1969
2. MULLINS CB, MASON DT, ASHBURN WL, et al: Determination of ventricular volume by radioisotope-angiography. *Am J Cardiol* 24: 72-78, 1969
3. STRAUSS HW, ZARET BL, HURLEY PJ, et al: A scintiphotographic method for measuring left ventricular ejection fraction in man without cardiac catheterization. *Am J Cardiol* 28: 575-580, 1971
4. ZARET BL, STRAUSS HW, HURLEY PJ, et al: A non-invasive scintiphotographic method for detecting regional ventricular dysfunction in man. *N Engl J Med* 284: 1165-1170, 1971
5. VAN DYKE D, ANGER HO, SULLIVAN RW, et al: Cardiac evaluation from radioisotope dynamics. *J Nucl Med* 13: 585-592, 1972
6. WEBER PM, DOS REMEDIOS LV, JASKO IA: Quantitative radioisotopic angiocardigraphy. *J Nucl Med* 13: 815-822, 1972
7. SECKER-WALKER RH, RESNICK L, KUNZ H, et al: Measurement of left ventricular ejection fraction. *J Nucl Med* 14: 798-802, 1973
8. STEELE PP, VAN DYKE D, TROW RS, et al: Simple and safe bedside method for serial measurement of left ventricular ejection fraction, cardiac output, and pulmonary blood volume. *Br Heart J* 36: 122-131, 1974
9. STEELE P, KIRCH D, MATTHEWS M, et al: Measurement of left heart ejection fraction and end-diastolic volume by a computerized, scintigraphic technique using a wedged pulmonary arterial catheter. *Am J Cardiol* 34: 179-186, 1974
10. HERMAN MV, GORLIN R: Implications of left ventricular asynergy. *Am J Cardiol* 23: 538-547, 1969
11. MASON DT, SPANN JF JR, ZELIS R, et al: Alterations of hemodynamics and myocardial mechanics in patients with congestive heart failure: Pathophysiologic mechanisms and assessment of cardiac function and ventricular contractility. In *Prog Cardiovasc Dis* 12: 507-557, 1970
12. DWORKIN HJ, GUTKOWSKI RJ: Rapid closed-system production of  $^{99m}\text{Tc}$  albumin using electrolysis. *J Nucl Med* 12: 562-565, 1971
13. ECKELMAN W, RICHARDS P, HAUSER W, et al: Technetium-labeled red blood cells. *J Nucl Med* 12: 22-24, 1971
14. MILLER RR, AMSTERDAM EA, BOGREN HG, et al: Electrocardiographic and cineangiographic correlations in assessment of the location, nature and extent of abnormal left ventricular segmental contraction in coronary artery disease. *Circulation* 49: 447-454, 1974
15. SANDLER H, DODGE HT: Use of single plane angiocardigrams for the calculation of left ventricular volume in man. *Am Heart J* 75: 325-334, 1968
16. MATIN P, KRISS JP: Radioisotopic angiocardigraphy: findings in mitral stenosis and mitral insufficiency. *J Nucl Med* 11: 723-730, 1970
17. BRAUNWALD E, LAMBREW CT, ROCKOFF SD, et al: Idiopathic hypertrophic subaortic stenosis: Description of the disease based upon analysis of 64 patients. *Circulation* 30: Suppl 4: 3-119, 1964
18. KING JF, DEMARIA AN, REIS RL, et al: Echocardiographic assessment of idiopathic hypertrophic subaortic stenosis. *Chest* 67: 723-731, 1973
19. MASON DT, BRAUNWALD E: Hemodynamic techniques in the investigation of cardiovascular function in man. In *Clinical Cardiopulmonary Physiology*, 3rd Ed, Gordon B, ed, Grune & Stratton, 1969, pp 153-170
20. ASHBURN WL, KOSTUK WH, KARLINER JS, et al: Left ventricular volume and ejection fraction determination by radionuclidic angiography. *Semin Nucl Med* 3: 165-176, 1973